

# Research on the Design of Chemical Manipulator Based on Torque Sensor

Xiaohui Li, Weiyuan Shi

Jinling Institute of Technology, Nanjing 211169, China  
[xiaohuili48239@126.com](mailto:xiaohuili48239@126.com)

To study the application of torque sensor for the joint design of chemical manipulator and realize the integrated design of the elastic body and signal processing circuit. Based on a new type of torque sensor with lightweight manipulator flexible joint, a three-dimensional model of elastic structure is built on this basis and then the finite element analysis is conducted on this design. The finite element analysis of Workbench is used and it can be seen from the simulation results that the elastomer structure design can effectively meet the strength requirements of chemical materials. It can be discovered from the calibration and testing of the sensor designed in this paper that the new torque sensor has good static characteristics and can well meet the usage requirement of flexible joints.

## 1. Introduction

In recent years, with the development of science and technology, the level of social mechanization has become higher and higher and robots have become more and more aware of the outside world. The use of torque sensors can better perceive the force of robots on the outside and good interactive communication can also be realized. Through the combined use of torque sensor and manipulator, the role of the kinetic model of manipulator can be played to timely detect the friction and collision between the manipulator and surrounding objects. And then, the effective protection measures can be taken timely to effectively improve the service security of the manipulator.

The design and research of the chemical manipulator based on the torque sensor in this paper is mainly aimed at the joint of service manipulators in the chemical industry. The structure is relatively simple, which can realize the integrated operation of the elastomer and the signal processing circuit and achieve the purpose of lightening the structural design. At the same time, this paper also focuses on how to effectively detect the collision phenomenon between the chemical manipulator and surrounding objects with the use of torque sensors.

## 2. Literature review

Since the first Shuttle Remote Manipulator System (SRMS) designed for space shuttles in Canada in 1981, Shuttle Remote Manipulator System has developed rapidly. It is mainly used to achieve the capture and delivery of satellites. It can also assist astronauts in their outbound activities. Sanponpute and Wattong proposed that its essence is to adjust the dynamic relationship between the robot's end force and position, so that the robot's end reaches the desired impedance characteristics. From an implementation point of view, impedance control is mainly divided into force-based impedance control and position-based impedance control (Sanponpute and Wattong, 2017). Qin et al. proposed a torque-free sensor solution based on an impedance control strategy for industrial robots to handle the problems of the robot in contact with the environment (including people). According to the experimental results, the program can quickly and accurately detect the external force and adjust the position loop and speed loop setting, so that the robot can follow the operator's intention to reach the target point when the operator drags the robot arm by hand. Based on this, it is possible to complete direct teaching of the torque-free sensor robot. Because the principle of the scheme is based on Cartesian space impedance control, only the robot's end position teaching can be taught, and the

robot's arbitrary posture teaching can't be achieved. In addition, due to the complex design of the observer and controller, it is necessary to make corresponding changes to the original robot controller, and it is also difficult to implement (Qin et al., 2016). Sun Y et al. proposed the use of real-time gravity and friction compensation to establish a virtual gravity-free and frictionless state, so that the robot can flexibly move under external forces to achieve direct teaching of the torque-free sensor (Sun et al., 2016). Previous FFC control with gravity and friction compensation is effective only for small robots, but it is difficult for large robotic arms to move under the human action due to their large inertia. In response to this limitation, Ji X et al. proposed to add inertial force compensation based on this, that is, FFC based on inertial force, gravity, and friction compensation (also known as FFC with independent compensation) (Ji et al., 2016). When compensating inertial force, gravity, and friction force, this method designs a compensation coefficient matrix for each of the three. In practical applications, it is also possible to adjust the smoothness of the movement of the robot during the teaching of external forces by compensating the coefficient matrix.

Zhang et al. studied sensors based on 12-dimensional force and acceleration information fusion and proposed 10 inertial parameters that can be used to identify the end load in real time with a 12-point sensor at the end of the robot. Including mass, center of mass, and inertia tensor, especially for objects with uncertain inertia in motion, such as water tanks, parts with holes, etc. After obtaining the inertia parameters of the load, the contact force between the end effector and the load or the environment can be identified based on the information of the acceleration sensor, and the inertia force item caused by the acceleration can be compensated (Zhang et al., 2016; Zhao et al., 2016). Jung et al. installed a wrist force sensor and an accelerometer at the end of the ABB robot to form a 12-dimensional sensor. Combined with the information of the joint encoder, a motion control strategy based on Kalman state estimation was proposed. It improved the motion control performance of the robot arm by accurately acquiring the real contact force in the Cartesian coordinate system (Jung et al., 2017). Borges also studied the impedance control strategy with acceleration closed loop, and they proposed an observation-based force and acceleration information fusion model. The experiment was performed on a Staubli RX60 industrial robot arm equipped with an ATI force/torque sensor, a linear accelerometer, and a gyroscope. Through experiments, it has been proved that in the transition of contact force, the use of force and acceleration fusion information can make the robot adapt to many non-deterministic models and unknown environments and improve the intelligence level of the robot (Borges et al., 2017).

At present, there are few studies on 12-dimensional sensors at home and abroad, and there are no mature reports. The American JR3 company has developed a 12-degree-of-freedom force sensor (6 force components and 6 acceleration components). The purpose is to compensate for the inertial force term in the six-dimensional force measurement. That is, the acceleration sensor is used to measure the six-dimensional acceleration when the object moves, and the inertial force is compensated by a certain algorithm to achieve the purpose of accurately recognizing the contact force.

Meng Ming et al. from Hefei institute of automation in China have proposed a force/torque sensor of 12 dimensions. The implementation method is to integrate a six-dimensional acceleration sensor based on a bi-ring film structure into a six-dimensional wrist force sensor, and the two sensors have the same coordinate system. Through the feedback compensation of the six-dimensional acceleration sensor, the true contact force between the end effector and the external environment can be separated from the six-dimensional wrist force sensor information.

In summary, the above-mentioned research work has done in-depth research on the limitations of mechanical space, mechanical machining errors, and the influence of a large number of strain gauges, etc. However, there are few studies on the application of robots. Therefore, based on the above research status, the method of torque compensation is mainly used to directly control the robot's torque. The direct teaching of the torque-free sensor is achieved by partial or complete dynamic torque compensation to provide or balance the torque required for the operator to drag the robot arm.

### **3. Design and research of chemical manipulators based on light-weight flexible joint torque sensors**

The torque sensor is usually installed on the output shaft of the sense joint motor of the manipulator, which is composed of a torque disk attached with the strain gauge and the corresponding signal processing circuit. The torque sensor used for the joint generally adopts the strain-type principle and achieves the measurement of torque through the transformation from resistance variation to electrical signal variation of the strain bridge.

#### **3.1 Design objectives**

According to the requirements of the flexible requirements of the light-weight arm joint and the requirements of the rated driving torque of the harmonic reducer, the design indexes are as shown in Table 1:

Table 1: Torque sensor design index

Torque sensor technical indicators	Torque sensor design requirements
Maximum load torque (N·m)	100
Stiffness (N·m·rad <sup>-1</sup> )	$\geq 10^4$
Linearity/%	$\leq 3$
Hysteresis/%	$\leq 5$
Repeatability error/%	$\leq 5$
Sensitivity/%	$\leq 0.1$
Other	Structure symmetrical temperature compensation

### 3.2 Design Schemes of Manipulator Structure

The structure of the torque sensor elastomer structure is various, most of which use a spoke structure, such as measuring the torque information by attaching strain gauges on two sides of four uniformly distributed strain girders, specifying that the strain gage on the same side of each strain girder forms a half-bridge or full-bridge circuit, so the final result can be output through the compensation by two bridge circuits, making the torque measurement information more accurate. In view of this, the elastomer structure designed in this paper also adopts the spoke structure, as is shown in Figure 1.

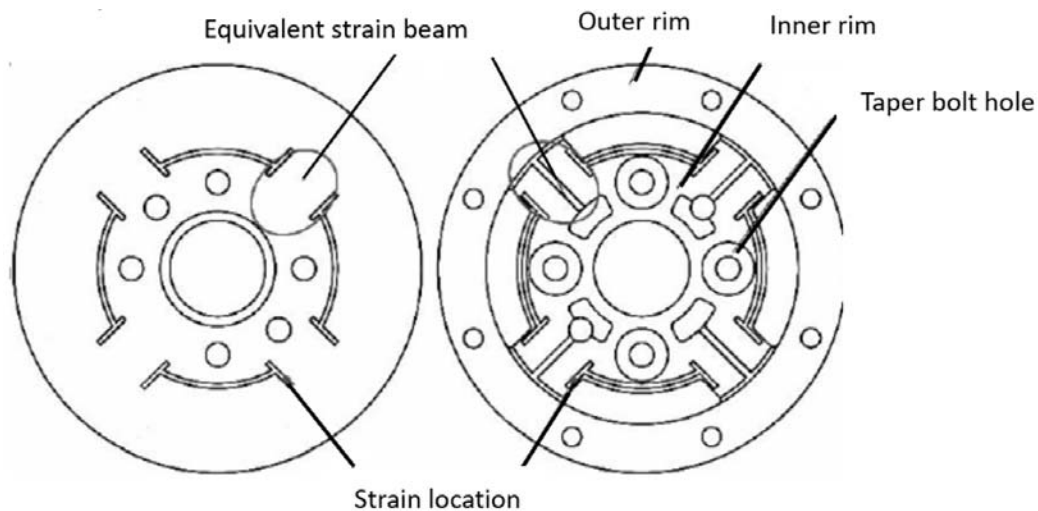


Figure 1: Elastomer structure chart

The resistance strain gauges are affixed symmetrically on the strain areas on both sides of the strain girder. Unlike the existing designs, the structure of four girders in the elastomer is not exactly the same. This paper adopts the same type of strain girders with different strength. The structure of two girders distributed in the 180° direction is the same and four girders are divided into two groups. The strain gauges on both sides of the same strain girder form a Wheatstone half bridge and the four strain gages of two strain girders distributed in the 180° direction form a full bridge circuit. There are two full bridge circuits in the torque sensor for the measurement. As long as there is one bridge circuit working in a normal state, the output of torque information can be guaranteed, which effectively increases the service life of the sensor. The input conical bolt hole of the elastomer in the inner rim and the output bolt hole in the outer rim. Considering the temperature compensation, the elastomer is symmetrical in the diagonal direction, which is also beneficial to improving the static characteristics and load capacity of the torque sensor. The non-hollowed part of the elastic strain zone is an equivalent strain girder, which can provide overload protection for the torque sensor. In addition, in the existence of the harmonic reducer in the flexible joint, the use of the torque sensor can reduce the impact of change in the harmonic steel wheels on the torque measurement.

### 3.3 Measurement scheme

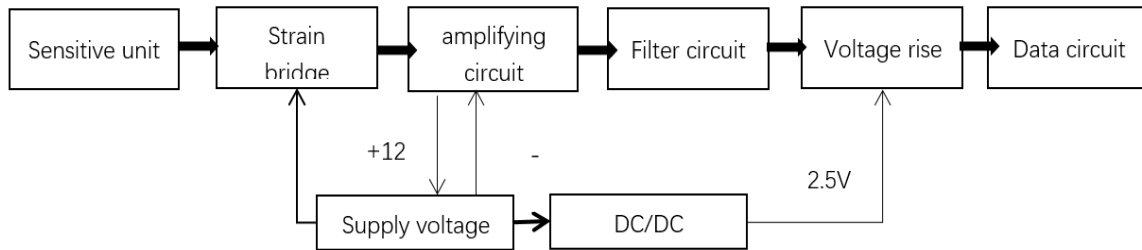


Figure 2: Measuring circuit system structure

The eight strain gages are divided into two groups according to the structure of the girder, forming two identical Wheatstone full-bridge bridge circuits. This circuit can help improve the static characteristics of the sensor, eliminate the temperature effect and the impact of load eccentricity and double the output voltage. The torque sensor measurement circuit board is installed inside the sensor to output the torque signal. The measurement circuit system structure is shown in Figure 2.

As the designed torque sensor has position installation requirements, the determination principle of the position of the strain gauge is: under the premise of ensuring the measurement accuracy, the sensitivity should be maximized.

### 3.4 Finite Element Analysis of Light-weight Flexible Joint Torque Sensors

The common manufacturing materials for torque sensors are aluminum alloy, beryllium bronze and stainless steel. Considering the processability, mechanical properties and quality, the aluminum alloys are more suitable, whose mechanical performance indexes are shown in Table 2:

Table 2: The main performance of hard aluminum material

Density(kg·m <sup>-3</sup> )	Poisson's ratio	Elastic Modulus/MPa	Shear modulus
2700	0.31	71000	27000

The mesh generation of the elastomer adopts the build-in automatic mesh generation function of the software. This mesh generation method can preferentially divide the elastomer into uniform tetrahedral meshes. The complex area can be designed for the elastomer structure, which can conducted the refined processing of the mesh and satisfies the requirements of statics analysis. Finally, 19246 nodes and 10946 units are obtained.

The conical bolt on the inner rim and the harmonic reducer are connected as the torque input of the sensor torque and the bolts evenly distributed on the outer rim and the rods are connected as the output. Apply torque loads of 20, 40, 60, 80, and 100 N to the circular surfaces on the input side of the conical bolt holes and apply fixed restraints on the circular surfaces of other rim bolt holes.

## 4. Analysis of the design results of light-weight flexible joint torque sensors

### 4.1 Sensitivity analysis

The sensitivity refers to the increment of the output signal of the sensor  $\Delta y$  and the increment of the output signal  $\Delta x$ . The limit value of the wallpaper is expressed as follow:

$$k = \lim_{x \rightarrow 0} \frac{\Delta y}{\Delta x} = \frac{dy}{dx} = y' \quad (1)$$

The calculation is conducted on this basis, the sensitivity of the different bridge circuits is actually basically the same. In actual measurement, only one bridge circuit is required to work. The design indexes of this paper require the sensitivity characteristics of the torque sensor to be lower than 0.1, which meets the design requirements.

## 4.2 Linearity analysis

The deviation between the measured input-output characteristic curve and the theoretical input-output curve is called the linearity of the sensor. The linearity definition formula based on the least-square method is as follows:

$$r_L = \pm \frac{\Delta L_{\max}}{y_{FS}} \times 100\% \quad (2)$$

Combined with the calibration data of the suspension bridge circuit, it can be concluded that when the torque load is 100 N·m in the counterclockwise loading process, the difference between the experimental value and the mean value is the largest and the difference between the positive and negative stroke reaches the maximum value, which is  $\Delta L_{\max}$ . The linearity under this occasion is  $\pm 1.0978\%$ . This figure shows that the hysteresis characteristics of the torque sensor required by this design index are less than 5%, which meets the design requirements.

## 4.3 Analysis of repeatability error

The reproducibility refers to the measured misalignment degree of multiple characteristic curves when the sensor changes continuously in the same direction under the same working condition. The formula is as follows:

$$r_R = \pm \frac{\Delta R_{\max}}{y_{FS}} \times 100\% \quad (3)$$

Combined with the record value of the bridge circuit calibration data, the above formula is used for calculation. The record value of the bridge circuit output voltage is shown in Table 3:

Table 3: Bridge circuit output voltage

BR	-100	-80	-60	-40	-20	0	20	40	60	80	100
1	0.40	0.75	1.25	1.70	2.10	2.50	2.90	3.30	3.70	4.15	4.60
2	0.40	0.80	1.15	1.60	2.05	2.50	3.00	3.40	3.80	4.20	4.60

It can be seen that in the counterclockwise loading process,  $\Delta R_{\max}$  reaches the maximum value with a load of 100 N·m and the maximum value is 62. On the other hand, in the clockwise deloading process, the  $\Delta R_{\max}$  reaches the maximum value with a load of 20 N·m the load and the maximum value is 26. Therefore, the value of  $\Delta R_{\max}$  is 62. It can also be concluded that the repeatability error of the torque sensor is  $\pm 1.347\%$  and this figure indicates that the designed index in this paper requires the repeatability error of the torque sensor to be less than 5% error and this requirement has been satisfied. Finally, the results of the calculations are organized and the linearity, hysteresis error, sensitivity and repeatability error of the two full-bridge circuits of the torque sensor are summarized.

Table 4: Torque sensor static indicator

Bridge circuit	Linearity	Sensitivity	Hysteresis	Repeatability
1	0.8261	0.0208	1.0978	1.3478
2	0.8328	0.0214	1.1012	1.3992

## 5. Conclusion

This paper designs a new type of mechanical joint torque sensor according to the application requirements of flexible joints for light-weight manipulators. At the same time, the three-dimensional model and simulation analysis are used to carry out the calibration experiments and the least square method is used to fit several important indexes of the torque sensor. Through the calibration test, the linearity, hysteresis error, sensitivity and repeatability error of the torque sensor designed in this paper all meet the design indexes, which verifies the correctness of the simulation results. The results show that the static index of the sensor satisfies the design requirements and that the structural design of the sensor is reasonable. The torque sensor provides real-time torque information for flexible joints, which can provide a theoretical basis for the research on the dynamic modeling control strategies of flexible joints.

Next, we should make full use of the information obtained by the torque sensor to perform force control and flexible control of the manipulator to enable it to complete more elaborate and advanced tasks in the chemical industry and provide better quality and safer service for the chemical production.

### Reference

- Borges J.C.S., Deus D.B.B.D., Filho A.C.L., Belo F.A., 2017, New contactless torque sensor based on the hall effect, *IEEE Sensors Journal*, (99), 1-1, DOI: 10.1109/JSEN.2017.2723041
- Ji X., Fan Y., Chen J., Han T., Cai P., 2016, Passive wireless torque sensor based on surface transverse wave, *IEEE Sensors Journal*, 16(4), 888-894, DOI: 10.1109/JSEN.2015.2499318
- Jung B.J., Kim B., Koo J.C., Choi H.R., Moon H., 2017, Joint torque sensor embedded in harmonic drive using order tracking method for robotic application, *IEEE/ASME Transactions on Mechatronics*, 22(4), 1594-1599, DOI: 10.1109/TMECH.2017.2694039
- Kim U., Lee D.H., Yong B.K., Seok D.Y., Choi H.R., 2017, A novel six-axis force/torque sensor for robotic applications, *IEEE/ASME Transactions on Mechatronics*, 22(3), 1381-1391, DOI: 10.1109/TMECH.2016.2640194
- Qin Y., Zhao Y., Li Y., You Z., Peng W., 2016, A high performance torque sensor for milling based on a piezoresistive mems strain gauge. *Sensors*, 16(4), 513, DOI: 10.3390/s16040513
- Sanponpote T., Wattong C., 2017, Torque transducer with check standard combination, 6(2), 59, DOI: 10.21014/acta\_imeko.v6i2.404
- Sun Y., Liu Y., Liu H., 2016, Temperature compensation for a six-axis force/torque sensor based on the particle swarm optimization least square support vector machine for space manipulator, *IEEE Sensors Journal*, 16(3), 798-805, DOI: 10.1109/JSEN.2015.2485258
- Zhang H.X., Ryoo Y.J., Byun K.S., 2016, Development of torque sensor with high sensitivity for joint of robot manipulator using 4-bar linkage shape, *Sensors*, 16(7), 991, DOI: 10.3390/s16070991
- Zhao F.J., Yan Q., Li B., Xie J.M., 2016, Workspace analysis of an over-constrained 2-RPU&SPR parallel manipulator, *Mathematical Modelling of Engineering Problems*, 3(2), 87-90, DOI: 10.18280/mmep.030208